

TenSense: IIoT Enabled Sensor Node for Remote Measurement of a Bolted Joint Tension

Michail Sidorov
*Department of Computer Science and
 Engineering*
Toyohashi University of Technology
 Toyohashi, Japan
 mike@usl.cs.tut.ac.jp

Phan Viet Nhut
*Department of Architecture and Civil
 Engineering*
Toyohashi University of Technology
 Toyohashi, Japan
 p175510@edu.tut.ac.jp

Atsushi Okubo
Toyo Metal Co., Ltd
 Toyohashi, Japan
 a-okubo@toyometal.co.jp

Yukihiro Matsumoto
Department of Architecture and Civil Engineering
Toyohashi University of Technology
 Toyohashi, Japan
 y-matsum@ace.tut.ac.jp

Ren Ohmura
Department of Computer Science and Engineering
Toyohashi University of Technology
 Toyohashi, Japan
 ren@tut.jp

Abstract — This paper presents a sensor node designed to measure the tension of a bolted joint for the purpose of unattended structural health monitoring. The electronic circuits are embedded inside a custom designed stainless steel washer. LoRa is used for wireless communication and data transfer between the sensor node and the base station. The proposed design eliminates the necessity of using specialized bolts with mechanical modifications to monitor tension making it an easy add-on to current and future mechanical structures. Design of the prototype is discussed and evaluated by means of simulation to confirm the proper functionality and adherence to the set requirements.

Index Terms — *Fastener Tension Monitoring, Structural Health Monitoring, Industrial Internet of Things, LoRa, Smart Metering*

I. INTRODUCTION

Bolts are widespread in the construction industry for making an easy and fast connection between different pieces or material. Bolted joint is a basic fastening method and is used in aircraft, building, bridge, etc. construction. The fastening procedure works by clamping two or more objects together using tension. This tension arises from rotary force or torque imposed on the fastener. Although the fastening method is easy and convenient, problems occur when the tension loosens. Once deployed, even if correctly assembled with enough pre-load applied to the fastener, bolted joints are susceptible to different kinds of stress making the joint lose its tension over time. Most common ones being vibration, shock and thermal expansion. In some cases the fastener itself may be susceptible to elongation process due to heavy load applied. For some applications it is critical to monitor this tension in order to know the general structural health and prevent the failure. Structures such as bridges, wind turbines, pipelines, aircrafts, etc. have to be properly designed and assembled. In order to ensure structural integrity it is vital to maintain it. Hence, scheduled inspections of bolted joints are performed to avoid failures. However, they can be costly and time consuming. Furthermore, it may not be convenient to perform inspections in places with limited access

to the structure. It is also possible for the fault to be unnoticed until critical damage to the bolted joint becomes apparent. To combat this problem the best solution is to use remote monitoring. While there are different designs proposed to monitor the tension of the fastener, further discussed in the related work section, most of them require either some mechanical modifications to the bolt itself [1], which in turn not only violate standards but also introduce unnecessary costs in manufacturing; are suited only for visual inspection [2]; or not suited for remote monitoring at all [3-4]. Hence, a need for an alternative solution arises. In order to combat these limitations we propose a smart sensor node capable of measuring and monitoring the tension of a bolted joint remotely by seamlessly integrating the design with an Industrial Internet of Things (IIoT) network.

The remaining of this paper is structured as follows:

- Section II lists the prototype requirements
- Section III reviews related designs proposed by other researchers or available on the market
- Section IV describes the design approach we take
- Section V describes the mechanical design and implementation part of the system
- Section VI describes the electronics design and implementation part of the system
- Section VII describes the software design
- Section VIII evaluates the performance of the proposed system in terms of simulation
- Section IX concludes the paper

Contribution of this work: TenSense, a sensor node for measurement of bolted joint tension with a novel washer design, seamless electronics integration and IIoT connectivity. Sensor data is collected by a base station and processed for an early failure diagnosis or predictive maintenance. In this paper the full system overview is presented. However, the design of the base station is not in its scope.

II. REQUIREMENTS

Our vision is to use the TenSense node on big sized structures, e.g. bridges, wind turbines, etc. Fig.1. These structures are sometimes placed in remote locations or are hard to get to in order to do inspections. Thus, a simple and practical solution is necessary. We have a made set of requirements that our prototype has to fulfill in order to distinguish itself from other designs, be more practical and appeal for industry use.

These are listed as follows:

- Sensor node has to have a small footprint. This will enable it to be used more conveniently.
- Tension sensing mechanism integration should require no modifications to be made to the bolt. Since bolts have to conform to a set standard any modifications done would mean an unacceptable deviation.
- Design should require no modifications to be made to the structure where it is intended to be used. Otherwise these modifications might have implications on the structure.
- Sensor node has to be targeted at unattended and remote monitoring via integration with IIoT.
- Ensure an operational life time of the sensor node equal to or greater than 5 years when transmitting once or twice per day.
- Use a low power and long range transmission protocol for communication. This is required both for extending the battery life and the communication distance between the base station and the sensor node.
- Implement collision avoidance mechanism to account for a scenario when a large number of sensor nodes transmit data to the base station. Although a small amount of packet loss is acceptable.
- Include the ability to reconfigure the node via OTA updates. A feature that is needed to comply with IIoT.

Basic functionality of the TenSense node is:

- Detect pre-tension degradation due to external and internal factors.
- Gather and transmit the above mentioned data for structural health monitoring and early maintenance

Hence, the motivation for this project is to create a sensor node that fulfills the requirements and functions stated above.

III. RELATED WORK

There are different techniques to monitor the tension of a bolted joint and we can split them into invasive or non-invasive.

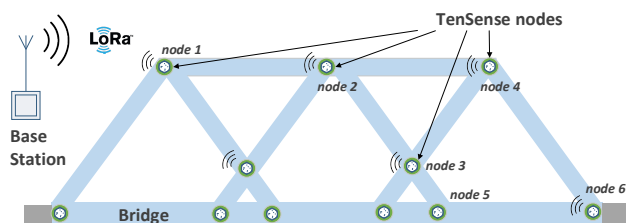


Fig. 1. TenSense application on a Girder Bridge

Invasive techniques usually include making modifications to the bolt in order to accommodate the tension sensing mechanism. Mekid et al. proposed a fastener tension monitoring system which requires the addition of a piezoelectric material to be incorporated into the core of the fastener [1]. This material acts as an energy source to power the electronic circuitry placed at the top of the bolt. However, this kind of invasive modifications will change the mechanical properties of the fastener and will make it more prone to elongation during fastening process due to the portion of the core being removed. Smith et al. proposed a tension monitoring systems with an RFID readout [5]. This, however, implies a very short communication range and is only suited for a close up inspection of the structure being monitored. Furthermore, a mechanical modification to the fastener itself is required. The system, being passive by nature, will only operate once the external signal from the interrogator is received. Another RFID based monitoring system developed by engineers working in NASA uses several washers, one being flat, other being spring type that acts as a switch mechanism to enable the RFID readout [2]. In case when there is not enough tension to compress the spring type washer, and in turn make an electrical connection, it is impossible to read the data from the RFID tag. This would indicate that the bolted joint either lost its tension and needs retightening or it has not enough pre-load.

Non-invasive ones require no modification to the bolt itself. Thus, an external sensor placement is needed. Mekid et al. proposed another type of monitoring system that uses a force transducer positioned between the bolts head and fastened surface [6]. The control circuitry, as in [1] is placed on top of the bolts head and is used to compare the measured tension to the pre-programmed threshold value. In case of any irregularities a signal is sent to the remote station to notify of this. A variation of the design proposed by Baroudi et al. includes an RF energy harvester to provide power to the control circuitry [7]. Both of these designs are split into two pieces and this approach introduces a certain degree of unpracticality. Furthermore, a chance of breaking the connection between the force transducer and the main control circuitry during application is very high.

Ohta et al. proposed to use a strain gauge to measure tension and either display measurements on a small screen or send them wirelessly [8]. This approach, however, requires to embed the utilized common silicon monocrystalline substrate together with dummy resistors that form a Wheatstone bridge inside the bolt implying that mechanical modifications to the bolt are necessary.

On a commercialized scale BoltSafe offers several washer products to monitor the tension of the bolted joint. One being continuous [4], where a measuring instrument has to be attached permanently, and another being periodic, where a probe needs to be attached to make a reading [3]. This approach is not suitable for remote monitoring, as the measuring equipment has to be in close proximity with the structure under test.

Another commercialized solution of monitoring the fasteners tension include a visual indicator, such as a dot that

changes color in response to the tension applied to the fastener. It is marketed under the name of SmartBolts [9] and this approach requires close visual inspection to be performed, thus, is not targeted at remote monitoring. However, a smart lid was proposed by Mekid et al. that attaches to the top of the bolt [10]. The lid has a color sensor and a wireless transmitter, enabling the color readout of the dot. The rest of the construction follows the design pattern described in [4-5].

Pulse-echo technique can also be used to measure the clamp load produced by the bolted joint. This approach requires an ultrasonic transducer to be placed on top of the bolt. Once active, an ultrasonic wave is then propagated through the bolt and reflected back for analysis. Some commercialized meters that utilize this technique are made by Dakota Ultrasonics, Norbar, Hydratight, etc. All of them have the same working principle and all of them share the same drawback – they are suitable only for close up checks. Wang et al. proposed another method which utilizes piezo sensors, one for generating an electrical wave on one side of the structure, propagating it to the other side and capturing it with a similar sensor. An interesting approach, however not applicable as the placement of the sensing elements requires them to be on different structures [11].

One more approach includes using a fiber-optic sensor that has a bragg grating, commonly known as FBG sensor. While these sensors do offer some benefits compared to the traditional ones e.g. stability over time, immunity to EMI and ability to measure ultra-fast events. However, these benefits would only be useful for very specific cases. Furthermore, while the sensor itself can have a small footprint, the electronics setup that is required to operate it has significant size and is not suited for small low power applications.

IV. APPROACH

Compared to all of the described products available on the market or proposed approach to monitor the fasteners tension eliminates the need of any modifications to the bolt itself as the whole design is incorporated into the structure of a custom designed washer. Most of the proposed designs by researchers in the previous section, that require bolt modification, neglected the fact that making those modifications to an already released product (bolt) would be a standard violation. Since large sized bolts are sold already with an integrated washer, we make no modifications to the set. Our sensor node will be used for a construction of big structures e.g. bridges, wind turbines, and is manufactured using stainless steel.

There are two important aspects to the design of a system that would fulfill the set criteria. One is mechanical, that ensures the custom washer has not lost its functionality, the other one – electronics. Thus, we have split them accordingly. The inner diameter of the washer is adapted to suit the M30 bolt type. Since these bolts come with an integrated washer as a set our designed washer does not replace it, but accompanies in order to conform to the standard. Our designed washer has a circular shape, however, the structure inside is split into several sections allowing to house the necessary electronics and power source components. This feature sets the design apart from the rest

available on the market as it allows for a seamless integration making it a true an all-in-one tension monitoring system.

V. MECHANICAL SYSTEM DESIGN AND IMPLEMENTATION

In order to settle down on the internal structure of the washer we had to find out whether making some parts of the washer hollow will affect the main function of the washer – being a washer. After a number of simulations of the stress distribution inside the washer with a certain number of cut out sections, we have settled down on a structure with six cut outs as the best possible solution. Detailed simulation results are provided in the evaluation section. The internal structure also defines the area available for the electronics, and can be seen in Fig. 2. It also shows the placement of the designed washer and its intended use with other components – bolt and a standard washer that comes as a set. Once the simulation confirmed the structural integrity of the washer the prototype was milled out of a stainless steel brick. Fig 3 shows one part of the washer. Depth of the cut outs is 5 mm, thus the height of the components, PCB and isolation between the electronic components and metal parts all have to fit within this 5 mm envelope. One of the sections is used for the main PCB, the rest is filled with batteries and strain sensing components.

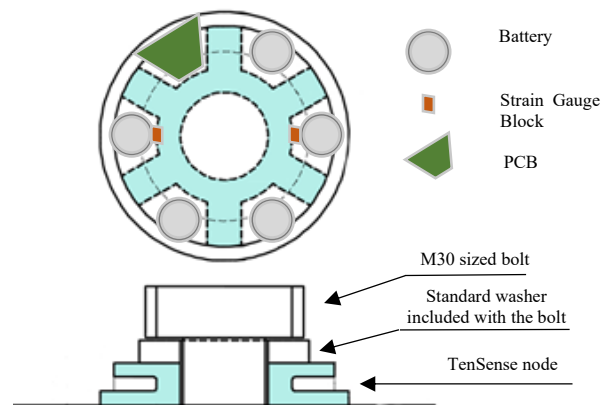


Fig. 2. Orthographic representation of the designed washer, top and side view, together with electronics component placement.



Fig. 3. One half of the TenSense node washer

VI. ELECTRONICS SYSTEM DESIGN AND IMPLEMENTATION

A. Communication Protocol comparison

For a device primarily dedicated to be used for IIoT choosing the correct communication standard is mostly application dependent. These applications include, but not limited to, are environmental monitoring, agriculture, smart cities, smart buildings, etc. The age we are living in is gearing towards the future where every electronic thing is interconnected with a single purpose of making our daily lives easier. Hence, a lot of researchers, developers and manufacturers have already jumped on the Internet of Things (IoT) wagon making this a self-fulfilling prophecy. IIoT is a subset of IoT mainly targeted for use in the industrial area. There are distinct features that set IIoT and IoT apart. Thus, even if an IoT device is designed to do the same things as IIoT device, it will not be classified as one. This is due to fact that IIoT devices have to meet higher operational standards in terms of security, scalability, reliability, serviceability and automation. The application by default defines the necessary hardware to be used for the design. Since devices targeted at IoT and IIoT need to use some kind of wireless communication means we need to look at currently available wireless standards. There are numerous ones competing on the market. To narrow them down to the necessary one it is feasible to split them according to the transmission range into several major groups – very short range, short range and long range. Very short range is dominated by RFID (Radio Frequency Identification), and NFC (Near Field Communication). Short range consists of ZigBee, Bluetooth (BLE) 5.0, 6LoWPAN (IPv6 over Low-power Wireless Personal Area Networks) and similar technologies. Whereas long range consists of cellular IoT protocols e.g. LTE-M, NB-IoT, and LPWAN e.g. SigFox, LoRa (short for Long Range) and RPMA. Many previous research papers compared different protocols suitable for IoT and IIoT in terms of coverage, transmission speed, etc [11–13]. However, all of this is heavily design and working environment dependent. Usually the most important aspect is omitted or vaguely mentioned – the power consumption of a transceiver module during the transmission (TX) sequence. Instead the trend is to specify battery life in years which is a vague indicator, since it depends on the battery capacity itself, transmission period, and the power management techniques implemented on software (sleep mode, etc.) and hardware levels. Hence, it is vital to look at the power consumption numbers at the System-on-Chip (SoC) level. Table I summarizes the important technical features of the most popular wireless IoT network protocols. Link budget heavily depends on the chip specification and transmit power used. Hence, the numbers will vary from one module to another. As can be seen there is quite a big spread in power consumption, depending on which LPWAN is chosen. Technologies like ZigBee, BLE 5.0, 6LoWPAN would offer smaller power consumption numbers since they provide a shorter communication range, e.g BLE requires 9.3 mA of current during TX while ZigBee and 6LoWPAN require 39.6 mA and 22 mA respectively [11–13]. However, all of them belong to a Personal Area Network type, and are not suited for long range communication. Therefore, let us look at technologies that provide long range communication. LTE-M is an evolution of LTE dedicated to IoT purposes. The name is a short abbreviation

of LTE-MTC that stands for LTE Machine-Type Communications. Since it relies on a cellular network for data transmission a SIM card needs to be used in the end device. Hence, this means an addition of unnecessary operational, installation and maintenance costs. NB-IoT is a further evolution of LTE-M, which caps the upload (UL) and download (DL) speeds, making it less heavy on LTE. Both LTE-M and NB-IoT operate at licensed bands, meaning some royalties need to be paid. In order to deploy a private network this might not be the best solution. Although the infrastructure is already in place, signaling for a convenient IoT device deployment, the power consumption of LTE-M and NB-IoT modems puts them at a clear disadvantage for devices that need to operate for years running of a small battery. The best candidates for our application are SigFox, RPMA and LoRa. The two former ones, however, have proprietary stacks and modules themselves consume a larger amount of power during transmission according to [12-13], [25]. Furthermore, SigFox has no data encryption. LoRa, on the other hand looks very attractive with the features that it provides and with the ability to deploy a private network it was chosen an optimum LPWAN candidate.

B. Tension measurement

Since there are many ways to measure tension we have to look at the most practical solution. Using an FBG sensor would inherently mean a need to design a complicated circuitry to power and process the data from the fiber optic sensor. Using a pulse-acoustic method would mean the placement of the transducer has to be outside of the washer, on top of the bolt to be precisely, otherwise it will not function correctly. For utilizing piezo sensors we would need to place them on two different structure parts, which clearly is not what we are aiming for. Thus, we take a traditional approach for tension measurement by utilizing bonded metallic strain gauges in the design. Strain gauges are constructed in a way that allows them change their electrical resistance in proportion to the amount of strain applied. They were used for these kind of measurements for over 50 years and are proven to be accurate if used correctly. This will to keep the cost down while providing the necessary measurement accuracy. Strain gauges can have different resistance. Usually the higher resistance gauge is preferred to be use. It has a lesser self-heating effect and can compensate for unwanted leadwire resistance. In order to read the output value of the strain gauge it needs to be set up in a correct way. Wheatstone bridge configuration is almost always used and it can have several variations depending on the number of strain gauges used, Fig. 4. Replacing one of the resistors with a strain gauge gives us a quarter bridge, replacing two of the gives us a half bridge. Full bridge consists of all resistors replaced by strain gauges. The latter two configurations can be used to increase the sensitivity of the circuit, albeit that depends on the placement of the gauges, as it is also possible to make one gauge to act as a dummy and use it only for temperature compensation. In a perfectly balanced configuration, the output of the bridge will theoretically be equal to 0 mV. Practically, due to tolerances there will be some voltage at the output. This can be dealt with in software providing some offset value to calibrate the initial reading to zero. Other sources of errors that can impact the measurement accuracy would be temperature drift and lead resistance.

TABLE I.
LPWAN PROTOCOL COMPARISON

Rating	LPWAN Protocols				
	<i>SigFox</i>	<i>LoRa</i>	<i>LTE-M (LTE Cat M1)</i>	<i>NB-IoT</i>	<i>RPMA</i>
Frequency Band	Sub-GHz region dependent ISM band 868, 902 MHz	Sub-GHz, region dependent ISM band LF: 160, 433 MHz, HF: 868, 915, 923 MHz	In-Band LTE	In-Band LTE, Guard Band LTE	Region independent 2.4 GHz ISM band
Module Current Consumption [14-18]	TX: 65 mA @ 13.5 dBm RX: 25 mA	TX: 47 mA @ 14 dBm RX: 21.5 mA	TX: 235 mA (avg) RX: not specified	TX: 255 mA (avg) RX: 81 mA (avg)	TX: 200 mA (min) RX: 75 mA (min)
Data Rate	12 bytes per message, 140 messages per day UL link only, no DL	0.3 to 37.5 kbps	UL: 0.2-1 Mbps DL: 0.2-1 Mbps	UL: 170 kbps DL: 250 kbps	UL: 78 kbps DL: 19.5 kbps
Modulation	D-BPSK and GFSK	LoRa and GFSK	DL: OFDMA, 16QAM UL: SC-FDMA, 16QAM	DL : OFDMA UL: SC-FDMA	DL: CDMA UL: RPMA
Coding	Ultra Narrow Band	Chirp Spread Spectrum	Direct-sequence spread spectrum (DSSS)	DSSS	DSSS (RPMA specific version)
Link Budget	154 dB	151 dB	146 dB	150 dB	>160 dB
Bandwidth	Total: 192 KHz 200 Hz for each device	HF band: 125, 250, 500 KHz LF band: 7.8, 10.4, 15.6, 20.8, 31.2 KHz	1.08 MHz	180 KHz	Total: 80 MHz, 1MHz on each channel side (up to 40ch)
Security	None	AES-128	RSA-2048	RSA-2048	AES-256
Typical Range	Rural: up to 50 km Urban: up to 10 km	Rural: up to 15 km Urban: up to 5 km	LTE coverage dependent	LTE coverage dependent	Urban: up to 15 km
Licensing or Fees	Fees per device and amount of data transmitted per day	NA	Cellular service fees	Cellular service fees	NA

Since the resistance of the gauge is affected by the temperature a second dummy gauge can be used to counter this as mentioned before. The effect of the lead resistance can be minimized by using a three lead wiring method. This, however, is best applicable when the gauge is placed farther away from other bridge elements, e.g. more than 1m away. In close proximity the lead effect is negligible. Hence, there is no need to employ for our application. The output voltage of the bridge is extremely low, hence it needs to be amplified. Typical configuration to drive the Wheatstone bridge consists of a voltage source and an operational amplifier to amplify the output signal. However, a one chip solution is used in our design.

C. LoRaWAN module choice

Wireless communication is taken care of by a LoRa module. A number of different ones are available on the market with different specifications. Table II provides important technical details that needed to be taken into consideration when choosing commercially available LoRa module as this choice critically affects the power consumption of the system. Data is compiled from respective datasheets [13], [26–28]. It is also worthy to note that while some chips are capable of LoRa modulation i.e. the PHY layer is present, they do not have the LoRaWAN MAC layer. Hence, they are limited in functionality. LoRaWAN has several classes as described in Table III. This class separation is done to address different needs required by various applications. All LoRaWAN devices have to have Class A implemented. Whereas Class B and C are extensions to Class A. The biggest difference between these classes is the time that device needs to listen for the uplink from the server. Class A devices have two slots open to receive the information, 1 and 2 seconds after the

uplink to the server is done. Class B adds scheduled receive windows and Class C keeps this window open indefinitely unless the device is in a transmit mode. Class C devices are considered to be more power hungry, due to this operational configuration. Using MAC commands is possible to configure the settings of an end node device, e.g. check status, change channel, SF factor, etc. Thus, it is a necessary addition to comply with IIoT requirements. Microchip, Multitech, RF Solutions, Murata and some other manufacturers produce LoRa or LoRaWAN certified modules. These modules are either a combination of a dedicated LoRa chip manufactured by Semtech with a simple microcontroller (MCU) to interface it, or just a module capable of using LoRa modulation. Hence, the main criteria for choosing the correct chip was power

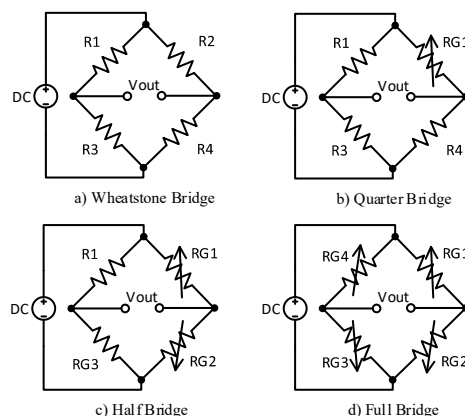


Fig. 4. Wheatstone bridge and strain gauge connection configurations

TABLE II.
LoRA AND LoRAWAN COMMERCIAL MODULE SPECIFICATION

Rating	Modules					
	<i>Microchip RN2903</i>	<i>USI</i>	<i>Murata</i>	<i>HOPE RFM95</i>	<i>MIPOT 32001353</i>	<i>Miromico FMLR</i>
RX Current	13.5 mA	10 mA	25 mA	10.3 mA	15 mA	15 mA
TX Current	124 mA @ 18.5 dBm	127 mA @ 18.8 dBm	128 mA @ 20 dBm	120 mA @ 20 dBm	70 mA @ 10 dBm	125 mA @ 20 dBm
Host MCU	None Control via UART	STM32L052 ARM Cortex-M0+	STM32L082 ARM Cortex-M0+	None Control via SPI	None Control via UART	STM32L151 ARM Cortex-M3
Radio Transceiver	RN2903	SX1272	SX1276	RFM95	SX1272	SX1272
LoRaWAN Class	A	A and C	A and C	Not	A and C	A
Form Factor in mm	17.8 x 26.7 x 3.34	12.0 x 13.0 x 2.0	12.5 x 11.6 x 1.76	16 x 16 x 1.8	15.5 x 26 x 3.16	14.0 x 22.0

TABLE III.
LoRAWAN CLASSIFICATION

Specification	Class		
	<i>A</i>	<i>B</i>	<i>C</i>
Bi-directional communication	Yes	Yes	Yes
Scheduled Receive Windows	No	Yes	Yes
Receive Window Frame	1s and 2s after UL	Configurable	Always Open

consumption coupled with physical dimensions. Most of the modules require the same amount of current to transmit at the highest TX level. However, both RN2903 and RF95 require a host controller, which in turn increases the valuable footprint of the PCB and the cost of adding an MCU. Whereas, both USI and Murata offer a complete solution, the documentation on the former one is sparse.

D. Main TenSense design

The full scale system consists of a large number of TenSense nodes and base station servicing them. Fig. 5 shows a simplified block diagram of our design. Each block plays its own distinct role. Since this is a distributed system we have the TenSense node itself and a gateway made using Raspberry Pi 3 (Rpi 3) to collect the information. RPi is only used for prototyping, it is possible to configure and use any other commercially available gateway. The purpose of it is to gather the sensor node data and make it available for access via internet.

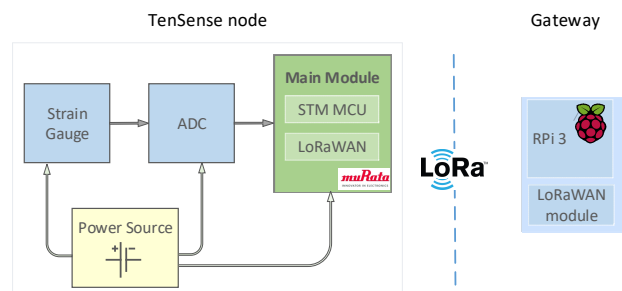


Fig. 5. Block diagram of the TenSense node

Strain gauge part as the name defines contains strain gauges configured in a Wheatstone bridge. By design it is possible to monitor the values from two different bridges. This is useful and helps account for the bending effect that may happen when one side of the fastener has a bigger preload than the other one. To implement this feature strain gauges are positioned on different sides of the washer, Fig. 2. The analog output from these blocks is conditioned using an HX711 Load Cell Amplifier chip and fed into the Murata CMWX1ZZABZ LoRaWAN module, the STM32 microcontroller integrated in the module to be precise. The circuitry is powered by coin cell batteries which by estimation provided in the evaluation section will last an adequate amount of time due to the power saving features implemented. Since the device will be used primarily for transmitting data and rarely for receiving, there is no need for it to support LoRaWAN Class B and C. Class A is fully sufficient to be utilized. Furthermore, there is no need for the load cell amplifier and strain gauge part to be operational all the time. Thus, in order to minimize the power consumption a simple power gating technique can be used where a component is completely disconnected from the power rail until it is needed again. This is done by including a MOSFET that acts as a simple switch and disconnects the HX711 from the power supply. The whole electronics assembly is covered by stainless steel making the placing of an antenna a critical issue. The early stage prototype utilized a ceramic chip antenna soldered to the PCB; Fig. 6, however, this is not an option to be used when integrating the PCB into the structure of a washer, as the surrounding stainless steel would unnecessarily load the antenna severely degrading its performance.

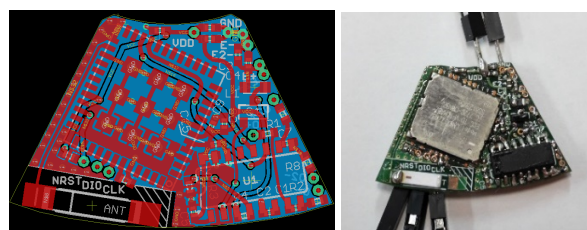


Fig. 6. PCB design and assembled board of an early TenSense node

One of the solutions is to use a simple external antenna. This, however comes with drawbacks as the antenna can be easily snapped off or damaged if handled improperly. Thus, an antenna has to be integrated into the structure of the sensor node. It was decided to place the antenna at the outer rim of the washer. A dedicated cut was made at the side of it to increase the distance between antenna and the metal structure of the washer. Fig. 7 shows the antenna shape and its placement. The simulation results are provided in the evaluation section.

VII. SOFTWARE DESIGN

From the operational point of view the software design is straight forward. Fig. 8 shows the simplified main loop. Most of the time the TenSense node will spend in sleep mode, since we only need to transmit once or twice per day. Thus, it needs to know when to wake up. The first time it enters the operational mode can be considered time 0, thus we can take this as the starting point for taking measurements and transmission. Real time clock (RTC) will help to keep the track of time and tell the main MCU when to wake up again to take the measurements. Since the LoRaWAN module allows to receive the data it is possible to reconfigure the TX time and period to suit the necessary scenario. Thus, the repetitive sequence consists of taking a measurement, transmitting it to the base station and entering the sleep mode until the RTC wakes up the system to repeat the same sequence all over again.

VIII. SYSTEM EVALUATION

There are two aspects to system evaluation. First one is the simulation necessary for the design process and second one is the physical module evaluation. Since the design is in its infancy, besides the simulation done that is a necessity for the

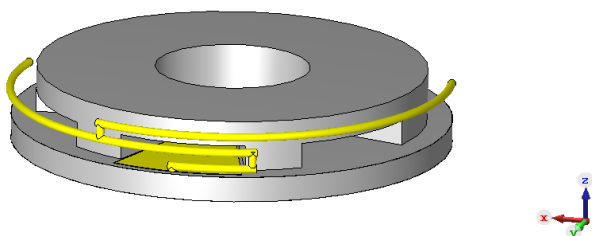


Fig. 7. Antenna Placement

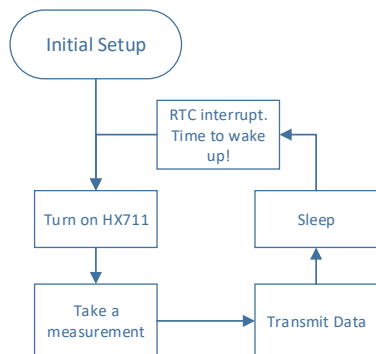


Fig. 8. Software flowchart

design process, the physical evaluation was performed on a basic level. Throughout evaluation requires a longer period of time and is will be covered in the future.

A. Investigation of the load carrying capacity of the washer

The following experiment investigates the stress distribution inside the designed washer once the pretension load is applied. Two types of washers are investigated: the solid one, that has no cutouts and the one used as a base for the TenSense node. The desired result of this experiment is to obtain a stress distribution in critical areas of a washer either similar to the solid washer or below the level of the yield strength specified for the stainless steel, i.e. the maximum level of stress that can be applied to the washer along its axis before it starts to permanently deform. Type of material chosen for the washer is austenitic stainless steel of grade 301 with a yield strength of 310 MPa. Obtaining stress distribution with lower numbers inside the designed washer than this value will prove that the structure will not deform under the pretension load. In order to investigate the load-carrying capacity of the washer, finite element analysis (FEA) was done using the LUSAS software package. Since we have symmetrical surfaces it was enough to use half models for the simulation. In this study, the applied load to the bolt represents the fasteners pretension load.

This load was assigned to the top surface of the washer. The value of the pretension load is 200 kN for the half model. Surface contacts were assigned to the standard washer and the main washer to evaluate their interaction. The following illustrates the wireframe model used for the simulation of a solid washer, Fig. 9, and the simulation results obtained, Fig. 10.

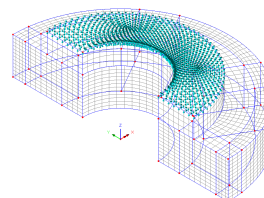


Fig. 9. Model used for stress simulation inside a solid washer

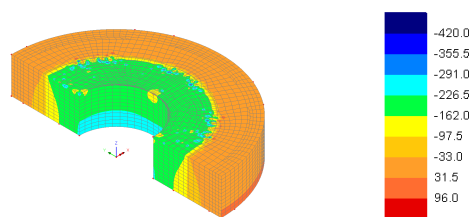


Fig. 10. Stress distribution in a solid washer

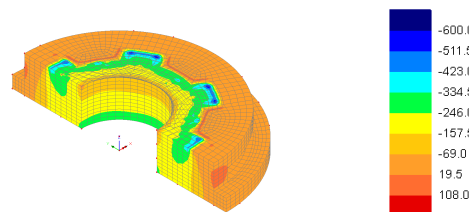


Fig. 11. Stress distribution in a washer with cut outs

Although a concentration of stress over 325 MPa is observed at some local points it is mainly due to the impact conditions specified in FEA model, Fig 10. Therefore, the solid washer is safe under the pretension load.

Same analysis was done for the TenSense washer. Fig. 11 illustrates the stress distribution in a final washer design with six cut outs. As with the previous simulation we can observe some concentrated local points with the stress over 325 MPa due to the same reason mentioned above. The general distribution is below 270 MPa. Thus, we can conclude that removing six predefined sections of a washer does not impact its main function – being a washer. To examine the results more closely the washer was split into three sections, namely top, middle and the bottom as illustrated in Fig. 12 a-c. We cannot observe anything out of the ordinary in the top or bottom parts of the washer as the stress is in the safe region, however, some interesting results can be seen in the middle part just at the edge of the cutouts, where it shows the middle portion of the washer with the stress level of more than 325 MPa. Although this can be alarming, as it is over the yield strength, the problem can be easily mitigated by creating arced edges during the construction process or simply by using a different type of steel with a higher yield strength.

B. Antenna performance evaluation

Antenna design and evaluation was performed using CST Microwave Studio 2017. This is suite is a very powerful tool for design, simulation and optimization of electromagnetic systems. Antenna was designed to have a custom shape since it is radiating in a close proximity to a metal construction. The resonant frequency target was set at 923 MHz. Time domain solver was used for the simulation, and settings are as follows: input impedance was normalized to 50 Ω, mesh type was set to

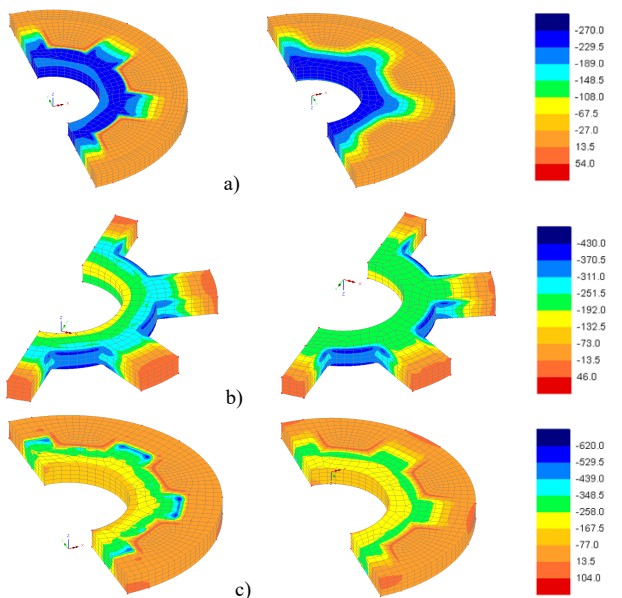


Fig. 12. Stress distribution in a) top part b) middle part c) bottom part of the custom washer. Left side – top view. Right side – bottom view.

hexahedral TLM, and accuracy was set to -50 dB. The results show that the center frequency of the antenna is 923.2 Mhz, Fig. 13a. with the VSWR value of 1.096, Fig. 13b. Bandwidth of the antenna by design is quite narrow, and is equal to 7.5 MHz, where VSWR value is below 1.5. Radiated efficiency is 75.5 %, Fig. 13c. The correct real world performance, however, needs to be confirmed once the sensor node is fully assembled, as it is usually the case with custom antenna designs that require a certain degree of tuning.

C. Battery life estimation

Since the TenSense node is powered by batteries and we can only use a certain number of them we need to estimate the average daily power consumption and calculate the required battery capacity, that would be sufficient to power the device for more than 5 years. This was done using the current consumption numbers compiled from the datasheets, Table IV, and a concrete transmission scenario. The average daily current draw can be found by using the following formula:

$$I_{Daily} = I_{ONmode} + I_{TXmode} + I_{sleepmode}$$

Where I_{ONmode} represents the amount of current consumed during tension measurement, when both HX711 and Murata

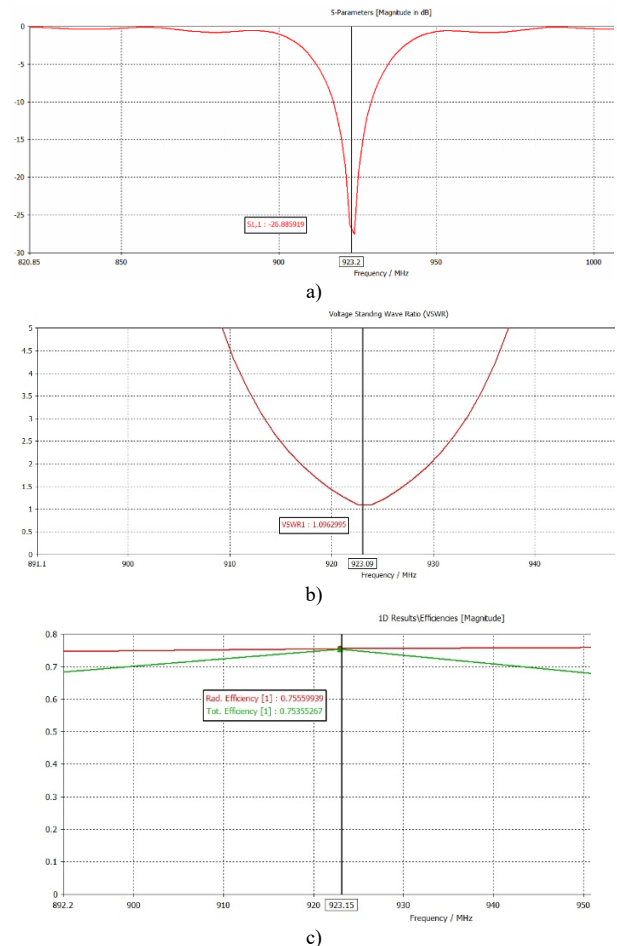


Fig. 13. Antenna Performance a) frequency b) VSWR c) efficiency

module are in operational mode. $I_{TX\ mode}$ is the current consumed during transmission time and $I_{sleep\ mode}$ is the current consumed during sleep sequence respectively. During sleep mode we only need to look at the current consumption of the main IC which consists of STM32 microcontroller and the Semtech SX1276 IC, since we turn off all of the unnecessary peripherals and enable them when needed. Assuming an extreme case, when a 20 dBm transmission power mode is used, the current consumption of the module during this sequence is around 128 mA. Transmission time will be one second (practically lower) and the time it takes to get a stable tension measurement would be three seconds. Thus, we get the following:

$$I_{ON\ mode} = (3.2 + 1.5) * \frac{3}{3600} = 0.0039\ mA$$

$$I_{TX\ mode} = 128 * \frac{1}{3600} = 0.035(5)\ mA$$

$$I_{sleep\ mode} = (0.00086 + 0.0002) * \frac{3596}{3600} = 0.00106\ mA$$

The total amount of current consumed per hour when the TenSense node is active is 0.03996 mA. However, rest of the day the node is in sleep mode. Thus, the daily consumption is the sum of daily active mode and daily sleep mode currents, and is equal to:

$$I_{daily} = 0.03996 + 0.02438 = 0.06434\ mA$$

In turn, the yearly current consumption is 24.48 mA. This number rises to 37.68 mA in case we decide to transmit twice per day. Our preliminary energy budget consists of 5 commercially available CR1625 Lithium batteries, with a capacity of 85 mAh each, Fig.2. Individually they are rated for low constant and pulse current drains from the connected load. Thus, connecting them in parallel will not only give us a budget of 425 mAh, but will also increase the overall constant and pulse currents. An addition of a supercapacitor will further help to buffer the energy needs during periods of short high current demand timeframes and will ease the load on a battery. Fig. 14 provides a rough estimate of the yearly current consumption depending on the number of times the TenSense node takes the measurement and transmits it per day. As expected the results show a linear correlation.

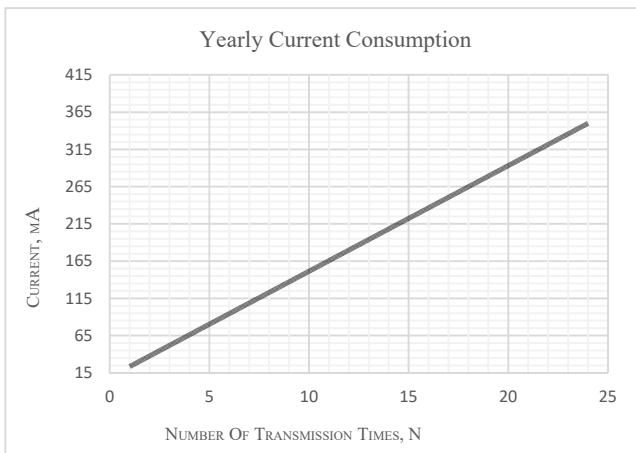


Fig. 14. Current consumption dependency on number of daily transmissions

TABLE IV.
CURRENT CONSUMPTION OF USED ICs

Specification	ICs		
	Murata LoRaWAN module		HX711
	STM32L082	SX1276	
On Mode	3.2 mA @ 16 MHz	1.6 mA	1.5 mA
Sleep mode	0.86 uA	0.2 uA	0 uA (power gated)
TX mode	128 mA		NA

Naturally we would like to extend the battery life for as long as possible. Thus, we need to limit the number of daily transmissions. If we transmit 5 times per day the battery life will be just over 5 years. However, if the transmission is limited to once per day the battery life expectancy rises to 18 years. This is only a rough estimation, as it does not account for the battery self-discharge and other factors that will degrade its life. Practically we aim to evaluate the real world performance figures of a TenSense node during a field test.

D. Basic system evaluation

Table V provides a basic system evaluation where we compare our system to some of the commercially available products and designs. As can be seen our proposed design provides a convenient and scalable solution for remote monitoring of a bolted joint tension.

TABLE V.
BASIC SYSTEM EVALUATION

Evaluation Criteria	System		
	TenSense	BoltSafe	Pulse-Echo Systems
Remote Monitoring	By design	Impossible	Impossible
External hardware requirement	Base station for data collection	All hardware for logging data	All hardware for logging data
Scalable	Yes	Not practical	Not practical
Battery lifetime	TX period dependent, max 18 years	NA	NA

IX. CONCLUSION

This paper presented a novel approach to measure the tension of a bolted joint remotely with all of the electronics integrated inside the custom designed washer. Numerous adjustments can be made to the design in order to improve performance figures. Thus, next iterations will focus more on circuitry optimization, power management techniques in order to maximize the battery life, and a better antenna design for a more efficient power transfer.

ACKNOWLEDGMENT

This project is done in collaboration with our industrial partner Toyo Metal Co., Ltd. (トヨーメタル株式会社)

REFERENCES

- [1] S. Mekid and U. Baroudi, "Fastener Tension Monitoring System," 8,893,557 B2, 2014.
- [2] G. Y. Lin, P. H. Ngo, T. F. Kennedy, and P. W. Fink, "RFID Torque Sensing Tag System For Fasteners," 9,483,674 B1, 2016.
- [3] BoltSafe, "BoltSafe Sensor PMS." BoltSafe Sensor Periodic Monitoring System datasheet, Version 2.0.
- [4] BoltSafe, "BoltSafe Sensor CMS." BoltSafe Sensor Continuous Monitoring System datasheet, Version 2.0.
- [5] J. D. Smith and S. G. Pothier, "Load Sensing System Including RFID Tagged Fasteners," 7,412,898 B1, 2008.
- [6] S. Mekid and B. Abdelhafid, "Bolt Tension Monitoring System," 8,596,134 B1, 2013.
- [7] U. Baroudi and S. Mekid, "Bolt Tension Monitoring System," 8,448,520 B1, 2013.
- [8] H. Ohta and T. Sumigawa, "Bolt with function of measuring strain," 7,293,466 B2, 2007.
- [9] Charles Popenoe, "Making The Case For Tension Indicating Fasteners," *Am. Fasten. J.*, 2011.
- [10] S. Mekid, B. Abdelhafid, and U. Baroudi, "Smart Lid for Smart Bolts and Probes," 8,540,468 B2, 2013.
- [11] T. Wang, G. Song, S. Liu, Y. Li, and H. Xiao, "Review of bolted connection monitoring," *International Journal of Distributed Sensor Networks*. 2013.
- [12] Y. Song, J. Lin, M. Tang, and S. Dong, "An Internet of Energy Things Based on Wireless LPWAN," *Engineering*, 2017.
- [13] K. Mekki, E. Bajic, F. Chaxel, and F. Meyer, "A comparative study of LPWAN technologies for large-scale IoT deployment," *ICT Express*, 2018.
- [14] R. S. Sinha, Y. Wei, and S. H. Hwang, "A survey on LPWA technology: LoRa and NB-IoT," *ICT Express*. 2017.
- [15] Texas Instruments, "A True System-on-Chip Solution for 2.4-GHz IEEE 802.15.4 and ZigBee Applications." CC2530F32, CC2530F64, CC2530F128, CC2530F256 datasheet, 2011.
- [16] STMicroelectronics, "Sub-GHz (868 or 915 MHz) low power programmable RF transceiver modules." 6LoWPAN SPhSGRF datasheet, 2017.
- [17] T. Instruments, "CC2642R SimpleLink™ Bluetooth® 5 low energy Wireless MCU." CC2642R datasheet, 2018.
- [18] WISOL, "Sigfox / Sub-1GHz." WSSF10R1AT datasheet, 2018.
- [19] Murata, "LoRa Module Data Sheet." CMWX1ZZABZ-TEMP datasheet, 2016.
- [20] Ublox, "Size and power optimized RPMA module for the Machine Network™." SARA-S200 datasheet, 2017.
- [21] DIGI, "Digi Xbee® Cellular LTE-M." LTE-M Cellular Smart Modem preliminary datasheet, 2017.
- [22] DIGI, "Digi Xbee® Cellular NB-IoT." NB-IoT Cellular Smart Modem preliminary datasheet, 2017.
- [23] Ublox, "NANO-S100 RPMA module." NANO-S100 datasheet, 2017.
- [24] USI, "WM-SG-SM-42 LoRa Module." USI LoRa Datsheet, 2017.
- [25] HOPERF Electronics, "RFM95/96/97/98(W) - Low Power Long Range Transceiver Module." RFM95/96/97/98(W) datasheet, 2017.
- [26] Microchip, "Low-Power Long Range LoRa® Technology Transceiver Module." RN2903 datasheet, 2018.